The Journal of Laryngology & Otology

cambridge.org/jlo

Variability of vestibular aqueduct measurements among axial, single-oblique and double-oblique computed tomography images

Y Quan[1], X J Gao[2], J Liu[3], R Z Gong[4], Q Wang[1], H Liang[1], J L Fu[1] and Q Cheng[1]

[1]CT room, Shanxian Central Hospital, affiliated with Jining Medical College, Heze, [2]Center of Laboratory Medicine, Yuhuangding Hospital, Yantai, [3]Department of Radiology, Weihai Central Hospital, affiliated with Weifang Medical College, Weihai and [4]Shandong Medical Imaging Research Institute, Shandong University, Jinan, PR China

Main Article

Dr R Gong takes responsibility for the integrity of the content of the paper

Cite this article: Quan Y, Gao XJ, Liu J, Gong RZ, Wang Q, Liang H, Fu JL, Cheng Q. Variability of vestibular aqueduct measurements among axial, single-oblique and double-oblique computed tomography images. *J Laryngol Otol* 2018;**132**:875–880. https://doi.org/10.1017/S0022215118001597

Accepted: 15 April 2018
First published online: 18 September 2018

Key words:
Vestibular Aqueduct;
Tomography, X-Ray Computed;
Temporal Bones; Diagnostic Imaging;
Dimensional Measurement Accuracy

Author for correspondence:
Dr Ruozhen Gong,
Shandong Medical Imaging Research Institute,
Shandong University,
No. 324, Jingwu Road, Jinan, Shandong
250021, PR China
E-mail: 2665709947@qq.com
Fax: +86 530 469 1777

Abstract

Objective. To investigate the morphology and dimensions of the vestibular aqueduct on axial, single-oblique and double-oblique computed tomography images.
Methods. The computed tomography temporal bone scans of 112 patients were retrospectively evaluated. Midpoint and opercular measurements were performed using axial, single-oblique and double-oblique images. Morphometric analyses were also conducted. The vestibular aqueduct sizes on axial, single-oblique and double-oblique images were compared.
Results. At the midpoint, the mean (± standard deviation) vestibular aqueduct measured 0.61 ± 0.23 mm, 0.74 ± 0.27 mm and 0.82 ± 0.38 mm on axial, single-oblique and double-oblique images, respectively; at the operculum, the vestibular aqueduct measured 0.91 ± 0.30 mm, 1.11 ± 0.45 mm and 1.66 ± 1.07 mm on the respective images. The co-efficients of variation of the vestibular aqueduct measured at the midpoint were 37.4 per cent, 36.5 per cent and 47.5 per cent on axial, single-oblique and double-oblique images, respectively; at the operculum, the measurements were 33.0 per cent, 40.5 per cent and 64.5 per cent. Regarding morphology, the vestibular aqueduct was fissured (33.5 per cent), tubular (64.3 per cent) or invisible (2.2 per cent).
Conclusion. The morphology and dimensions of the vestibular aqueduct were highly variable among axial, single-oblique and double-oblique images.

Introduction

An enlarged vestibular aqueduct is a commonly detected imaging abnormality in computed tomography (CT) evaluations of children with sensorineural hearing loss (SNHL).[1–3] Although the diameter of the aqueduct at the midpoint of the post-isthmic segment on axial images has been proposed as a potential diagnostic standard for an enlarged vestibular aqueduct, the measurement to be used as the standard remains inconsistent. The published values include 1.0 mm,[2] 1.4 mm,[4] 1.5 mm,[5–9] 1.9 mm[10] and 2.0 mm.[11] Moreover, one report did not refer to the midpoint width, but rather defined a large vestibular aqueduct as one with a 'visible large aperture (≥4 mm) and a small distance between the vestibule and traceable part of the vestibular aqueduct nearest to the vestibule (≥1 mm)'.[12] Another study considered the vestibular aqueduct to be enlarged if its diameter exceeded the diameter of one crus of the adjacent normal semicircular canal.[13] Though the causes of these inconsistencies remain unknown, they may be related to the course and morphology of the vestibular aqueduct, the technique used, and/or the site selected for measurement.

The vestibular aqueduct is a small bony canal that connects the vestibule to the cranial cavity. The vestibular aqueduct contains the endolymphatic duct and part of the endolymphatic sac. The shape of the vestibular aqueduct forms an inverted 'J', with a short ascending proximal segment and a longer distal descending segment. The proximal segment arises from the medial wall of the vestibule. As the aqueduct turns inferiorly, it narrows into an isthmus. The distal straight segment (i.e. the post-isthmic segment) enlarges along its inferior and posterior course, and ends as the external aperture on the posterior surface of the petrous pyramid.[14] Although the post-isthmic segment forms a triangular slit,[14] it is known that the vestibular aqueduct can appear tubular on routine axial images and images acquired in the 45° oblique plane.[14] Currently, its appearance on other types of images remains unknown.

To date, most of the reported CT imaging data of the vestibular aqueduct have been based on measurements obtained on routine axial sections, with only a few studies examining the vestibular aqueduct using other types of sections.[15,16] However, axial sections are not ideal for assessing the anatomy and dimensions of the vestibular aqueduct owing to its oblique orientation. Thus, assessing the morphology of the vestibular aqueduct in other planes is essential. The present study aimed to identify and characterise the morphology of the vestibular aqueduct on axial, single-oblique and double-oblique CT images.

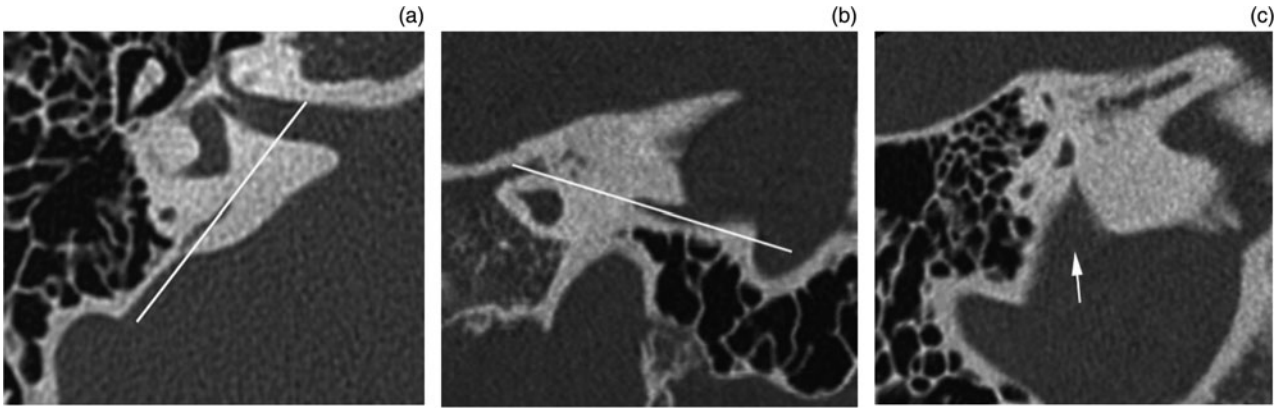

Fig. 1. Single-oblique and double-oblique images of the vestibular aqueduct. (a) Orthogonal axial reference image shows the reconstruction of the single-oblique image (white line) through the midpoint of the vestibular aqueduct. (b) Single-oblique image shows the reconstruction of the double-oblique image (white line) through the vestibular aqueduct. (c) Double-oblique image depicts normal anatomy of the vestibular aqueduct (arrow). The vestibular aqueduct was considered fissured because it was funnel-shaped in the double-oblique image, but tubular in the axial and single-oblique images.

Materials and methods

Study population

Institutional research ethics review board approval was obtained for this study. Patient anonymity was maintained.

A search of our institution's medical records and radiology databases for consecutive patients who underwent CT scans of the temporal bone for reasons other than SNHL and vertigo attacks, from July 2009 through January 2011, revealed 115 patients. Patients were excluded if they had undergone previous surgery on the temporal bone that made the vestibular aqueduct difficult or impossible to identify ($n = 1$), or if the CT images were of poor quality ($n = 2$). The remaining 112 patients (62 men and 50 women; 224 ears), with a mean (± standard deviation (SD)) age of 41.76 ± 18.89 years (age range, 1–77 years), comprised our study population.

The CT examinations were performed for the following indications: otitis media ($n = 33$), trauma ($n = 5$), cholesteatoma ($n = 51$), conductive hearing loss ($n = 11$), mastoidectomy follow up ($n = 5$), facial nerve paralysis ($n = 1$), headache ($n = 1$), otalgia ($n = 2$), foreign bodies in the external acoustic meatus ($n = 1$) and external otitis ($n = 2$). We then assessed the audiological records of all the patients to ensure that none of them had SNHL.

Computed tomography scan protocol

All of the subjects were scanned with a 16-section, multidetector CT scanner (Somatom Sensation 16; Siemens Medical Solutions, Forchheim, Germany). The head of each subject was placed in a neutral position, without chin tilt, to approximate the Reid base line. Both temporal bones were covered by the original scan. The axial images were acquired with the following parameters: slice thickness, 0.6 mm; increment, 0.3 mm; 120 kV; 150–350 mAs; pitch, 0.8; reconstruction kernel, B70; matrix, 512 × 512; and field of view, 300 mm. The image dataset was reconstructed to an 80 mm field of view, with an individual voxel size of 0.6 × 0.6 × 0.6 mm. Then, we used a workstation (Wizard; Siemens Medical Solutions) to obtain the multiplanar reformation images.

Data post-processing

The archived images in the Digital Imaging and Communications in Medicine format were transferred to a separate workstation (Volume; Siemens Medical Solutions). The images were rendered anonymous, with all clinical data, including the patients' histories, removed. The images were presented in random order.

Because the proximal segment of a normal vestibular aqueduct is usually invisible, we used the distal segment for measurements. The single-oblique images were generated from the axial images by positioning the reference line through the midpoint of the vestibular aqueduct (Figure 1a). The double-oblique images were generated from the single-oblique images by positioning the reference line through the vestibular aqueduct (Figure 1b). The double-oblique images depict the normal anatomy of the vestibular aqueduct (Figure 1c). The single-oblique and double-oblique images for each ear were independently generated at the workstation by two radiologists (YQ and RG, with 6 and 16 years of experience with temporal bone CT images, respectively). The anatomical locations and orientations of the structures to be evaluated were confirmed on images in the axial and coronal planes of reference. The time required to post-process the CT image datasets was 2–3 minutes per ear.

Post-isthmic aqueduct measurements

The methodology for measuring the vestibular aqueduct was adapted from Vijayasekaran *et al.*[17] and Dewan *et al.*[18] (Figures 2 and 3). The images were magnified, and then we obtained two measurements of the aqueduct on each plane: a measurement at the approximate midpoint and a measurement at the external aperture. The measurements were manually obtained and calculated to the nearest 0.01 mm using electronic calipers. The measurements were performed by two radiologists (YQ and RG) and the averaged value was regarded as the final value.

Midpoint measurement

The midpoint of the vestibular aqueduct in the axial, single-oblique and double-oblique images was defined as the part of the vestibular aqueduct located half of the distance in the petrous bone from its origin in the labyrinth to its aperture in the epidural space (Figure 2). We used the posterior wall of the vestibule or the crus commune in place of the origin of a normal aqueduct if the aqueduct was invisible. Measurements were obtained on the image with the largest midpoint width.

https://doi.org/10.1017/S0022215118001597 Published online by Cambridge University Press

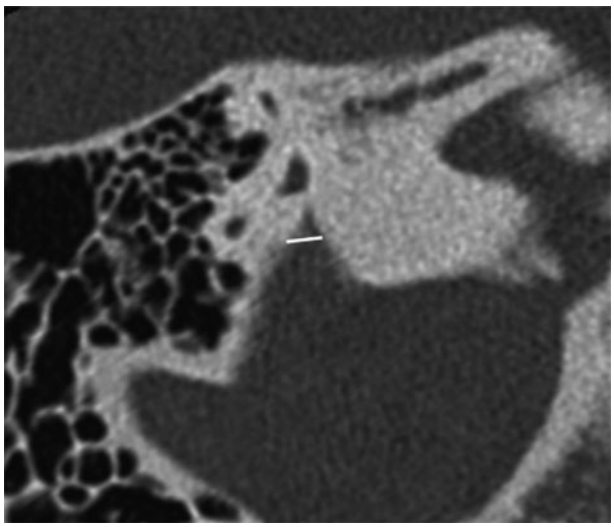

Fig. 2. The midpoint widths of the vestibular aqueduct are defined as the part of the vestibular aqueduct located half the distance in the petrous bone from its origin in the labyrinth to its aperture in the epidural space. The posterior wall of vestibule, or crus commune, was used in place of the origin of a normal aqueduct if it was invisible. The midpoint was measured on the image in which the width was largest.

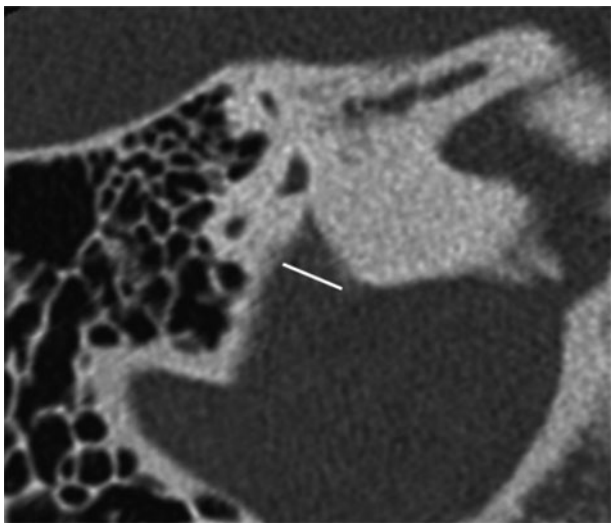

Fig. 3. The opercular widths of the vestibular aqueduct are measured by drawing a line from the opercular edge anterolaterally to form a 90° angle with the posterior wall of the petrous bone.

Opercular measurement

The opercular widths of the vestibular aqueduct were measured in the same plane by drawing a line from the opercular edge anterolaterally to form a 90° angle with the posterior wall of the petrous bone (Figure 3). Measurements were obtained on the CT image with the largest opercular width.

Morphology

We designated the vestibular aqueduct as funnel-shaped in terms of morphology when the size of the operculum was two times larger than the size of the midpoint in any one of the three image types. The vestibular aqueduct was considered invisible if it was difficult or impossible to identify on all of the axial, single-oblique and double-oblique images. The vestibular aqueduct was considered fissured if it was funnel-shaped in any one of the three image types, but tubular in the other two image types (Figure 1). The vestibular aqueduct was considered tubular if it was shaped like a tube in all of the axial, single-oblique and double-oblique images (Figure 4).

Statistical analysis

Numerical data are reported as means ± SDs. We compared the size of the vestibular aqueduct among the axial, single-oblique and double-oblique images using the Kruskal–Wallis test. If a significant difference was identified among the three image types, post-hoc pairwise comparisons were then performed using the Mann–Whitney U test with Bonferroni correction. Inter-observer agreement was assessed with the intraclass correlation co-efficient. Intraclass correlation co-efficient values of 0.41–0.60, 0.61–0.80, and 0.81 or higher indicated moderate agreement, substantial agreement and almost perfect agreement, respectively. In addition, the 95 per cent confidence intervals were assessed. The co-efficient of variation (equal to the SD divided by the mean) was calculated for each image type and anatomical location. The chi-square test was used for comparing categorical variables. Statistical analyses were performed with SPSS 16.0 software (IBM, Chicago, Illinois, USA) and GraphPad Prism software version 5.00 (San Diego, California, USA). Differences were considered significant at $p < 0.05$.

Results

The vestibular aqueduct measurements for each image type are presented in Table 1, and Figures 5 and 6.

A significant difference was identified in the size of the vestibular aqueduct as measured at the midpoint among the axial, single-oblique and double-oblique images (Kruskal–Wallis test). Post-hoc pairwise comparisons revealed statistically significant differences between the image types. Moreover, a significant difference in the size of the vestibular aqueduct as measured at the operculum was noted among the three image types. Post-hoc pairwise comparisons reached statistical significance.

The co-efficients of variation for the measurements obtained on the three image types are provided in Table 2. The co-efficients of variation were largest for the midpoint and operculum measurements obtained on the double-oblique images.

There was substantial agreement between the two radiologists for the midpoint measurements obtained using axial, single-oblique and double-oblique images (Table 3). The two readers had almost perfect agreement for the operculum measurements obtained using axial, single-oblique and double-oblique images (Table 3). The high inter-observer agreement for the midpoint and operculum measurements obtained on all image types implies good reproducibility.

Table 4 summarises the vestibular aqueducts according to morphological type in the axial, single-oblique and double-oblique images. None of the aqueducts appeared funnel-shaped on the axial images.

Statistically significant differences in the morphological types were observed among the axial, single-oblique and double-oblique images ($p < 0.001$). Further analyses revealed that the morphological types differed significantly between the axial and single-oblique images ($p = 0.006$), between the axial and double-oblique images ($p < 0.001$), and the between single-oblique and double-oblique images ($p < 0.001$).

Examinations of the gross morphology on the CT images showed that tubular morphology was the most prevalent (144 out of 224; 64.3 per cent), followed by the fissured (75 out of 224; 33.5 per cent) and invisible (5 out of 224; 2.2 per cent) morphologies (Table 5).

https://doi.org/10.1017/S0022215118001597 Published online by Cambridge University Press

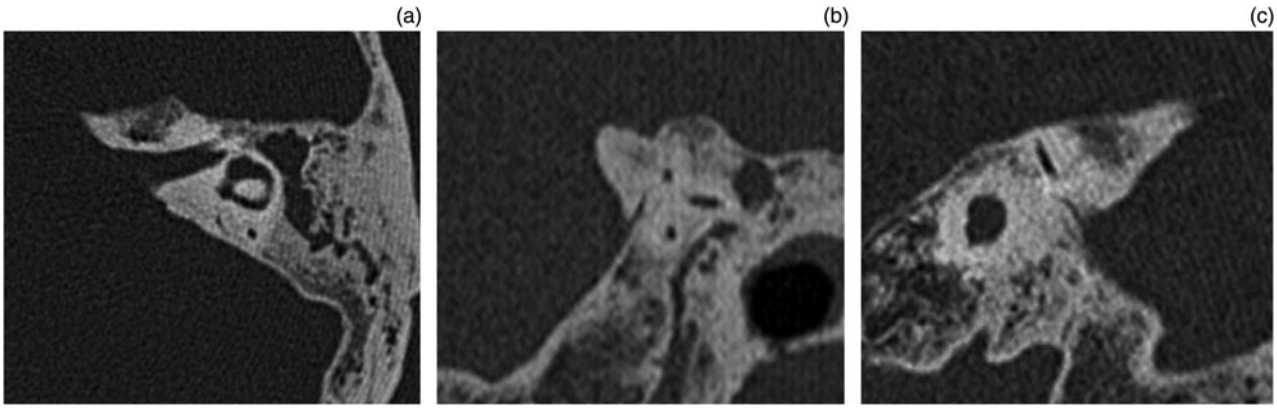

Fig. 4. The vestibular aqueduct was considered tubular because it was shaped like a tube in all of the (a) axial, (b) single-oblique and (c) double-oblique images.

Table 1. Vestibular aqueduct size at midpoint and operculum, on axial, single-oblique and double-oblique images*

Anatomical location	Axial image	Single-oblique image	Double-oblique image
Midpoint	0.61 ± 0.23 (0–1.10)	0.74 ± 0.27 (0–1.40)	0.82 ± 0.38 (0–2.35)
Operculum	0.91 ± 0.30 (0–1.55)	1.11 ± 0.45 (0–3.20)	1.66 ± 1.07 (0–5.40)

Data represent the mean ± the standard deviation (and range), in millimetres. *Total of 224 ears

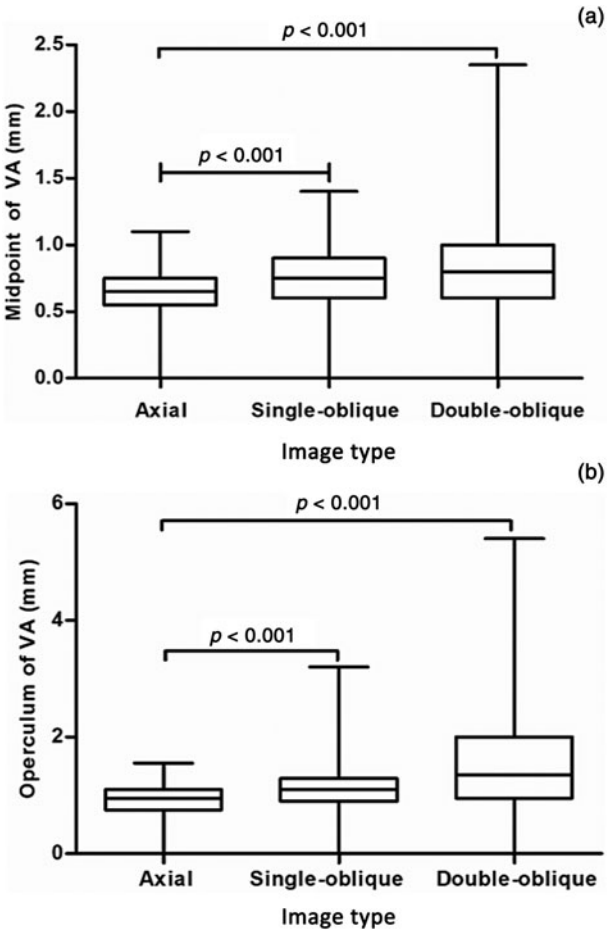

Fig. 5. Box plots show the size of the (a) midpoint and (b) operculum measured in the axial, single-oblique and double-oblique images. The boundaries of the box plots indicate the 25th and 75th percentiles, and the whiskers indicate the minimum and maximum (range) of all values. The line within each box indicates the median. Vestibular aqueduct size was compared between the two groups using the Mann–Whitney U test with Bonferroni correction. VA = vestibular aqueduct

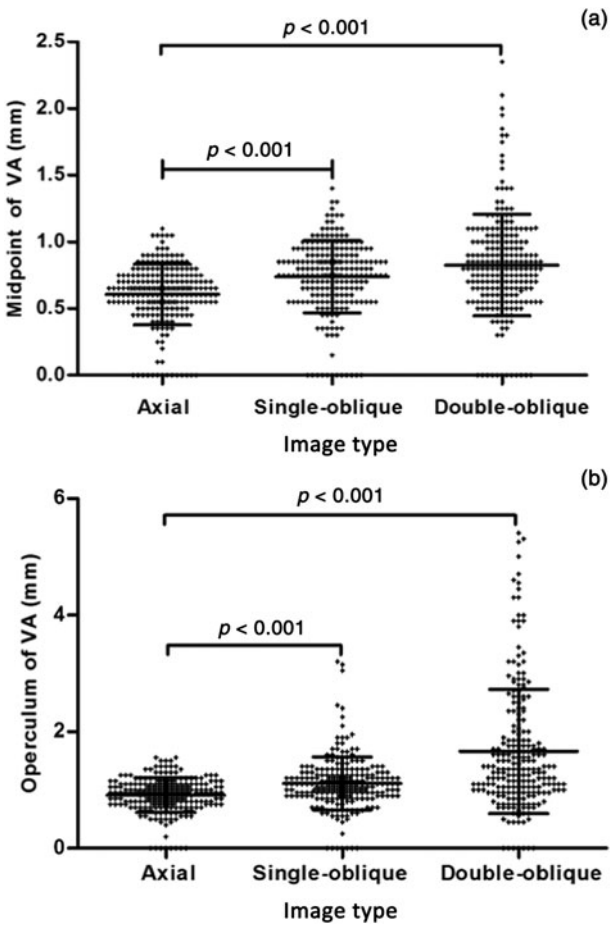

Fig. 6. Scatter dot plot for the size of the (a) midpoint and (b) operculum of 224 ears measured in the axial, single-oblique and double-oblique images. The middle line within each cluster of dots indicates the mean. The lines above and below indicate the mean ± standard deviation. '+' indicates the value of the size of the (a) midpoint and (b) operculum. Vestibular aqueduct size was compared between the two groups using the Mann–Whitney U test with Bonferroni correction. VA = vestibular aqueduct

https://doi.org/10.1017/S0022215118001597 Published online by Cambridge University Press

Table 2. Co-efficients of variation for measurements obtained on each image type

Anatomical location	Axial image	Single-oblique image	Double-oblique image
Midpoint	37.4	36.5	47.5
Operculum	33.0	40.5	64.5

Data presented in percentages

Table 3. Intraclass correlation co-efficients for vestibular aqueduct measurements, for each image type

Anatomical location	Axial image	Single-oblique image	Double-oblique image
Midpoint	0.77 (0.71–0.82)	0.72 (0.65–0.78)	0.78 (0.73–0.83)
Operculum	0.85 (0.83–0.89)	0.82 (0.78–0.86)	0.90 (0.87–0.92)

Data in parentheses are the 95 per cent confidence intervals

Table 4. Numbers of vestibular aqueducts of each morphological type, on axial, single-oblique and double-oblique images

Morphology	Axial image	Single-oblique image	Double-oblique image	Total
Funnel-shaped	0	10	65	75
Tubular	219	209	154	582
Invisible	5	5	5	15
Total	224	224	224	672

Table 5. Numbers of vestibular aqueducts according to gross morphology on CT images

Morphology	Vestibular aqueducts (*n* (%))
Fissured	75 (33.5)
Tubular	144 (64.3)
Invisible	5 (2.2)
Total	224

CT = computed tomography

Discussion

The present study demonstrated that the morphology and dimensions of the vestibular aqueduct vary greatly depending on whether the evaluations are performed using axial, single-oblique or double-oblique images.

In an adult, the vestibular aqueduct has an inverted 'J' appearance, with a short ascending proximal segment and a longer distal descending segment. The proximal segment arises from the medial wall of the vestibule, and curves superiorly and medially into a bend, which is the narrowest portion of the aqueduct; this segment is called the isthmus and it corresponds to the bend. The distal straight segment enlarges along its inferior and posterior course, and ends as the external aperture on the posterior surface of the petrous pyramid.[6,15,19] The isthmus is the narrowest segment of the aqueduct, measuring 0.3 mm in diameter.[14] The outer aperture of the aqueduct measures approximately 2.0–6.0 mm in the larger diameter and 1.0 mm in the shorter diameter.[14]

Here, the size of the operculum was largest when measured on double-oblique images (1.66 ± 1.07 mm), followed by single-oblique (1.11 ± 0.45 mm) and axial (0.91 ± 0.30 mm) images (Table 1). This finding is in agreement with results reported previously.[14] Lo *et al.* reported that seeing the entire endolymphatic sac on a single section requires double-oblique reformation at 70° from the infraorbital-meatal plane and 45° from the sagittal plane.[20] Because of the oblique orientation of the aqueduct, axial, coronal and sagittal images are differently angulated from its long axis. Single-oblique images are partially consistent with its oblique orientation. However, double-oblique images are completely consistent with its oblique orientation. Thus, double-oblique images show more of the vestibular aqueduct on a single section than do axial images. This explains why the size of the operculum was largest when measured on double-oblique images.

In the current study, the vestibular aqueduct measurements varied the most when using double-oblique images, but had little variability when using axial images. Our results showed that the SDs for both the midpoint and operculum measurements were largest when using double-oblique images (0.38 and 1.07, respectively), followed by single-oblique (0.27 and 0.45, respectively) and axial (0.23 and 0.30, respectively) images. A large SD indicates that the data points are far from the mean, while a small SD indicates that they are clustered closely around the mean. Indeed, the co-efficients of variation for the midpoint and operculum measurements were largest for the double-oblique images (47.5 per cent and 64.5 per cent, respectively). These findings confirm high variance in the size of the vestibular aqueduct when measured on double-oblique images, while the vestibular aqueduct measurements on axial and single-oblique images have low variance.

In terms of the morphology of the aqueduct, we found that the tubular form was the most prevalent (64.3 per cent), followed by the fissured (33.5 per cent) and invisible (2.2 per cent) forms. Moreover, the prevalence of each morphological type differed depending on whether axial, single-oblique or double-oblique images were utilised. In total, 75 ears (33.5 per

https://doi.org/10.1017/S0022215118001597 Published online by Cambridge University Press

cent) had a fissured aqueduct and 144 ears (64.3 per cent) had a tubular aqueduct in our study (Table 5). We considered the vestibular aqueduct to be fissured if it was funnel-shaped in any one of the axial, single-oblique or double-oblique images, but tubular in the other two image types. In fact, the fissured morphology is in agreement with the three-dimensional anatomy of the aqueduct. However, as mentioned above, the tubular morphology was the most prevalent, and this high prevalence may be related to our categorisation.

In addition, most of the vestibular aqueducts were found to be tubular on axial images. This is likely because the plane of axial images is inconsistent with the axis of the vestibular aqueduct. When the plane of the CT image is consistent with the axis of the vestibular aqueduct, then the vestibular aqueduct will usually appear as funnel-shaped in morphology.

Several limitations of our study should be noted. First, we did not examine whether age had an effect on or was related to the vestibular aqueduct measurements. However, prior studies by Vijayasekaran *et al.*[17] and Legeais *et al.*[21] reported that the size of the vestibular aqueduct was unrelated to age. Thus, it is unlikely that age affected our findings. Second, it was difficult to demonstrate the fissured morphology on single-oblique and double-oblique images, particularly as we positioned the reference lines through the midpoint of the vestibular aqueduct; hence, the proximal segment of the vestibular aqueduct was non-linear. This may have resulted in an underestimation of the prevalence of the fissured morphology in our subject population. Finally, our study lacked anatomical measurements of the vestibular aqueduct. However, we can suppose that axial measurements of the aqueduct on axial CT images should be slightly larger than the anatomical measurements, as axial images are significantly angulated from the axis of the aqueduct.

- An enlarged vestibular aqueduct is a common imaging abnormality in computed tomography evaluations of children with sensorineural hearing loss
- The vestibular aqueduct diameter at the post-isthmic segment midpoint on axial images is a potential diagnostic standard for an enlarged vestibular aqueduct
- Because of the oblique orientation of the vestibular aqueduct, axial, coronal and sagittal images are differently angulated from its long axis
- Single-oblique images are partially consistent with its oblique orientation, but double-oblique images are completely consistent
- The vestibular aqueduct morphology and dimensions were highly variable among axial, single-oblique and double-oblique images
- Regarding aqueduct morphology, the tubular form was most prevalent (64.3 per cent), followed by fissured (33.5 per cent) and invisible (2.2 per cent) forms

Conclusion

Our results revealed high variability in the morphology and dimensions of the vestibular aqueduct among axial, single-oblique and double-oblique images.

Competing interests. None declared

References

1 Mafong DD, Shin EJ, Lalwani AK. Use of laboratory evaluation and radiologic imaging in the diagnostic evaluation of children with sensorineural hearing loss. *Laryngoscope* 2002;**112**:1–7
2 Boston M, Halsted M, Meinzen-Derr J, Bean J, Vijayasekaran S, Arjmand E *et al.* The large vestibular aqueduct: a new definition based on audiologic and computed tomography correlation. *Otolaryngol Head Neck Surg* 2007;**136**:972–7
3 Madden C, Halsted M, Benton C, Greinwald J, Choo D. Enlarged vestibular aqueduct syndrome in the pediatric population. *Otol Neurotol* 2003;**24**:625–32
4 Zalzal GH, Tomaski SM, Vezina LG, Bjornsti P, Grundfast KM. Enlarged vestibular aqueduct and sensorineural hearing loss in childhood. *Arch Otolaryngol Head Neck Surg* 1995;**121**:23–8
5 Valvassori GE, Clemis JD. The large vestibular aqueduct syndrome. *Laryngoscope* 1978;**88**:723–8
6 Swartz JD. An overview of congenital developmental sensorineural hearing loss with emphasis on the vestibular aqueduct syndrome. *Semin Ultrasound CT MR* 2004;**25**:353–68
7 Dahlen RT, Harnsberger HR, Gray SD, Shelton C, Allen R, Parkin JL *et al.* Overlapping thin-section fast spin-echo MR of the large vestibular aqueduct syndrome. *AJNR Am J Neuroradiol* 1997;**18**:67–75
8 Berrettini S, Forli F, Bogazzi F, Neri E, Salvatori L, Casani AP *et al.* Large vestibular aqueduct syndrome: audiological, radiological, clinical, and genetic features. *Am J Otolaryngol* 2005;**26**:363–71
9 Koesling S, Rasinski C, Amaya B. Imaging and clinical findings in large endolymphatic duct and sac syndrome. *Eur J Radiol* 2006;**57**:54–62
10 Arcand P, Desrosiers M, Dubé J, Abela A. The large vestibular aqueduct syndrome and sensorineural hearing loss in the pediatric population. *J Otolaryngol* 1991;**20**:247–50
11 McClay JE, Tandy R, Grundfast K, Choi S, Vezina G, Zalzal G *et al.* Major and minor temporal bone abnormalities in children with and without congenital sensorineural hearing loss. *Arch Otolaryngol Head Neck Surg* 2002;**128**:664–71
12 Okumura T, Takahashi H, Honjo I, Takagi A, Mitamura K. Sensorineural hearing loss in patients with large vestibular aqueduct. *Laryngoscope* 1995;**105**:289–93
13 Weissman JL. Hearing loss. *Radiology* 1996;**199**:593–611
14 Minerva B. Oral cavity and oropharynx. In: Mafee MF, Valvassori GE, Becker M, eds. *Imaging of the Head and Neck*, 2nd edn. Stuttgart: Thieme, 2005;**686**
15 Ozgen B, Cunnane ME, Caruso PA, Curtin HD. Comparison of 45 degrees oblique reformats with axial reformats in CT evaluation of the vestibular aqueduct. *AJNR Am J Neuroradiol* 2008;**29**:30–4
16 Murray LN, Tanaka GJ, Cameron DS, Gianoli GJ. Coronal computed tomography of the normal vestibular aqueduct in children and young adults. *Arch Otolaryngol Head Neck Surg* 2000;**126**:1351–7
17 Vijayasekaran S, Halsted MJ, Boston M, Meinzen-Derr J, Bardo DM, GreinwaldJ *et al.* When is the vestibular aqueduct enlarged? A statistical analysis of the normative distribution of vestibular aqueduct size. *AJNR Am J Neuroradiol* 2007;**28**:1133–8
18 Dewan K, Wippold 2nd FJ, Lieu JE. Enlarged vestibular aqueduct in pediatric sensorineural hearing loss. *Otolaryngol Head Neck Surg* 2009;**140**:552–8
19 Pyle GM. Embryological development and large vestibular aqueduct syndrome. *Laryngoscope* 2000;**110**:1837–42
20 Lo WW, Daniels DL, Chakeres DW, Linthicum Jr FH, Ulmer JL, Mark LP *et al.* The endolymphatic duct and sac. *AJNR Am J Neuroradiol* 1997;**18**:881–7
21 Legeais M, Haguenoer K, Cottier JP, Sirinelli D. Can a fixed measure serve as a pertinent diagnostic criterion for large vestibular aqueduct in children? *Pediatr Radiol* 2006;**36**:1037–42

https://doi.org/10.1017/S0022215118001597 Published online by Cambridge University Press